Longitudinal dynamics of laser-cooled fast ion beams: square-well buckets, space-charge effects, and anomalous beam behaviour

M. Weidemüller,* B. Eike, U. Eisenbarth, M. Grieser, R. Grimm, I. Lauer, P. Lenisa, V. Luger, M. Mudrich, U. Schramm,† and D. Schwalm

Max-Planck-Institut für Kernphysik, 69029 Heidelberg, Germany

Abstract. We present recent results of our experiments on laser cooling of fast stored ion beams at the Heidelberg Test Storage Ring. The longitudinal motion of the ions is directly cooled by the light pressure force, whereas efficient transverse cooling is obtained indirectly by longitudinal-transverse coupling mechanisms. Laser cooling in novel bunch forms consisting of square-well buckets leads to longitudinally space-charge dominated beams. The observed longitudinal ion density distributions can be well described by a self-consistent mean-field model based on a thermodynamic Debye-Hückel approach. When applying laser cooling in square-well buckets over long time intervals, hard Coulomb collisions suddenly disappear and the longitudinal temperature drops by about a factor of three. The observed longitudinal behaviour of the beam shows strong resemblance with the transition to an Coulomb-ordered ion string.

I INTRODUCTION

Laser cooling is the method-of-choice for the crystallization of ion clouds confined at rest in ion traps [1–4]. The resonant light pressure acting on the ions provides an extremely strong damping force resulting in very low temperatures. At these low temperatures, the plasma parameter Γ, defined as the ratio of the Coulomb potential energy between nearest neighbor ions to the thermal kinetic energy per ion, becomes larger than one already at moderate densities. For a one-component plasma with $\Gamma > 1$, a phase transition into a Coulomb ordered state takes place. At $\Gamma \simeq 1$, a one-dimensional Coulomb string of ions can be formed, whereas for two- and three-dimensional system, the phase transition to the crystalline state occurs at $\Gamma \gg 1$.

Although storage rings confining ions with large speed share many common features with ion traps (except their size, of course), there is, at present, no unambiguous proof for ion beam crystallization [5,6]. One may wonder why laser cooling of fast ion beams in storage rings, as introduced about ten years ago [7–10], did not immediately lead to the observation of beam crystallization. Two main reasons have so far prevented the attainment of crystalline ion beams by laser cooling: the forces exerted on the ions by the ring lattice in co-operation with the huge beam energy lead to extreme heating rates [11], and direct transverse laser cooling of a fast ion beam is practically impossible. In addition, destructive effects by the ring lattice, such as shear in the bending sections of the ring, will break any kind of Coulomb-ordered structure except the linear string and possibly zig-zag bands [a].

In the course of the last year, we have made important progress in laser cooling towards crystalline beams at the Heidelberg Test Storage Ring (TSR) which has led us to new intriguing observations. On the one hand, we have introduced a novel method for indirect transverse cooling based on a single-particle interaction of

*) E-mail: m.weidemueller@mpi-hd.mpg.de

†) Permanent address: Ludwig-Maximilians-Universität München, Sektion Physik, 85748 Garching, Germany

a) For specific ring lattices, this restriction can be overcome by special cooling schemes designed to provide constant angular velocity (see, e.g. Refs. [12] and [13]). First experimental efforts into this direction are reported in Ref. [14], but the conditions necessary for constant angular velocity seem hard to be met experimentally.

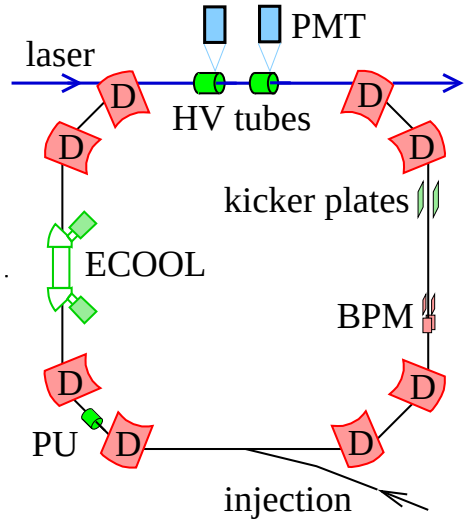

FIGURE 1. Schematic view of the Heidelberg Test Storage Ring (TSR) with its basic elements relevant for laser cooling. The laser beam is merged at one of the straight section of the TSR. The ion beam is bunched by applying an RF voltage to the longitudinal kicker plates. D: bending dipole magnets; not shown are the twenty focusing quadrupole magnets. ECOOL: electron cooler; BPM: beam profile monitor; PU: electrostatic pickup; HV tubes: high-voltage biased drift tubes; PMT: photomultiplier tubes.

ions with the laser light [14]. The method provides true 3D laser cooling, and transverse cooling rates are significantly improved as compared to indirect transverse cooling methods used earlier [15], especially when applied to dilute ion beams. On the other hand, we have developed novel bunch forms based on square-well buckets for very efficient laser cooling over long time intervals which are only limited by the beam lifetime. In Sect. II, we review the essential features of longitudinal and transverse laser cooling at the TSR. In Sect. III, we present results of our experiments on laser cooling in square-well buckets yielding longitudinally space-charge dominated beams. In Sect. IV we report the sudden disappearance of hard Coulomb collisions of a dilute laser-cooled ion beam. Our observations show that we are now entering a qualitatively new, interesting regime. Sect. V finally gives a brief discussion of our results in view of future developments.

II LASER COOLING AT THE TSR

Our experiments towards Coulomb ordering are performed with $^9Be^+$ ions which are injected into the TSR at a beam energy of 7.3 MeV. The initial beam current after multiturn injection is typically 0.3 μA corresponding to about 10^7 ions in a beam of several centimeters in diameter. The $1/e$ storage lifetime is typically 25 s at a residual pressure in the ring chamber of about 5×10^{-11} mbar. The TSR with its basic elements is schematically depicted in Fig. 1. The ion beam is precooled by electron cooling. Within a few seconds, the electron cooling leads to a decrease of the longitudinal temperature from typically 5000 K to about 300 K (relative momentum spread $\delta p/p \sim 10^{-5}$). The transverse equilibrium emittance after electron cooling is about $10^{-2}\,\pi$ mm mrad which corresponds to an ion beam diameter of about 1 mm. Electron precooling thus provides excellent starting conditions for subsequent laser cooling.

A Longitudinal laser cooling

Laser cooling relies on the radiation pressure exerted by resonant laser light on the ions [16]. The light force arises from repeated momentum transfer in a series of many absorption–spontaneous emission cycles. The alkali-like $^9Be^+$ provides a strong dipole-allowed transition line in the near-UV spectral range (D_2 line $2^2S_{1/2} \rightarrow 2^2P_{3/2}$ at a restframe wavelength of 313.13 nm). As shown in Fig. 1, the laser beam is merged copropagating with the ion beam in one of the straight sections of the storage ring over a length of about 5 m (corresponding roughly to 1/10 of the ring circumference $C = 55.4$ m). In the laboratory frame, the resonance

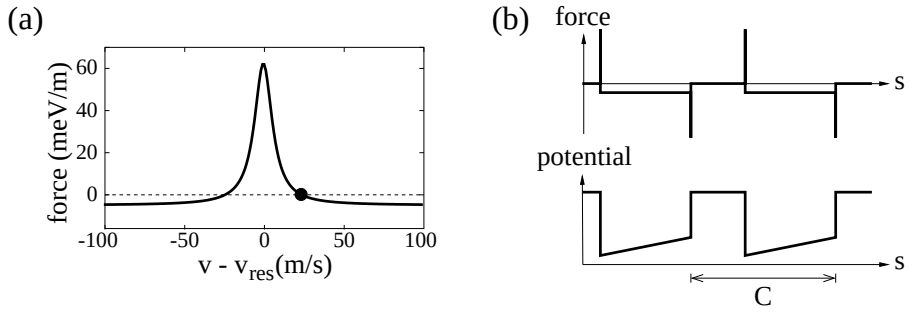

FIGURE 2. (a) Light-pressure force plus velocity-independent counterforce as a function of the velocity v relative to the resonant velocity $v_{\rm res}$. The dot indicates the stable force equilibrium at the velocity v_*. (b) Bunching force and resulting pseudopotential as a function of the longitudinal coordinate in the comoving frame s for a square-well bucket providing a constant counterforce. C denotes the ring circumference ($C = 55.4\,\mathrm{m}$).

wavelength is Doppler-shifted to 300.35 nm at the chosen ion beam energy corresponding to a velocity of $\beta = 0.0417$. This particular choice of the velocity allows us to use powerful fixed-frequency argon ion lasers. Due to the hyperfine structure of the D_2 line, two laser frequencies separated by 1.30 GHz are required to realize a closed excitation cycle. The total power of the UV laser beam in the interaction region is typically 60 mW focussed into a diameter of about 2 mm yielding a considerable saturation of the transition. The resulting maximum radiation-pressure force amounts to approx. 60 meV/m averaged over the storage ring round trip.

The Doppler effect leads to a very sharp dependence of the radiation-pressure force on the ion velocity. The resonance width corresponding to typically 20 m/s determines the capture range of the light force. To obtain stationary conditions over long time intervals, the accelerating laser force has to be counteracted by an additional, oppositely directed force (counterforce). The combination of these two forces as depicted in Fig. 2 (a) provides friction along the longitudinal degree of freedom necessary for ion beam cooling, i.e. damping of the momentum fluctuations in the frame moving at the mean velocity. Different schemes have been demonstrated to create the counterforce [7,17–19]. Here, we will concentrate on laser cooling of bunched ion beams [17,19], where the counterforce is provided by a longitudinal radio-frequency field tuned to a harmonics of the ion's revolution frequency (225 kHz under our conditions). The RF field applied to the non-resonant kicker device (see Fig. 1) confines the longitudinal ion motion in so-called RF buckets. In Fig. 2 (b), a square-well bucket with counterforce is shown as a specific example which is will be discussed in Sect. III A.

Intrabeam Coulomb scattering (IBS) leads to bimodal longitudinal velocity distributions of the laser-cooled ions: a very cold ($T \simeq 10\,\mathrm{K}$) fraction of ions experiencing the strong friction force, and a hot ($T \simeq 1000\,\mathrm{K}$) background of ions that have undergone a large longitudinal momentum change by a close Coulomb collision [20]. These momentum changes is much larger than the capture range of the light force. Besides providing a counterforce, longitudinal confinement in RF buckets has the additional advantage to recycle ions into the laser-cooling process after they have undergone a close Coulomb collision. The most effective longitudinal cooling scheme to date is a combination of RF bunching with recently developed extensions of the capture range through broadband laser excitation [20,21]. Attainable damping times in our experiments, referring to a $1/e$ reduction of the longitudinal mean kinetic energy in the comoving frame, are below 1 ms, i.e. two to three orders of magnitude faster than achievable damping times with electron cooling.

In the experiments presented here, the capture range extension is based on the ion excitation through optical rapid adiabatic passage accompanied by the corresponding momentum transfer. This process offers a much broader dependence on the ion velocity than resonant excitation [21]. Rapid adiabatic passage is realized by applying appropriate voltages to the HV tubes indicated in Fig. 1. The induced local change in the ion velocity is equivalent to fast switching of the laser frequency in the ion's rest frame which leads to the desired adiabatic excitation of the ion.

B Transverse laser cooling

The momentum transfer between the merged ion beam and laser beam is restricted to the longitudinal degree of freedom. Direct transverse laser cooling is known to work very efficiently for slow atomic beams [16] and

has been proposed for fast ion beams by several authors [22–24]. In the reality of a storage ring, however, implementation of the proposed schemes for direct transverse cooling appears to be extremely difficult, mainly due to two effects related to the high ion velocities: First, the interaction times for transverse laser irradiation are very short, and second, first-order Doppler shifts make the atomic resonance extremely sensitive to slightest angular misalignments between ion beam and laser beam.

In contrast to direct transverse cooling, *indirect* methods for transverse laser cooling have successfully been demonstrated [18,19,14]. To extend the longitudinal light force to also damp the tranvserse degrees of freedom, one has to find appropriate mechanisms to couple longitudinal and transverse motion. One coupling mechanism is provided by a dense ion beam itself, namely longitudinal-transverse thermal relaxation through intrabeam Coulomb scattering as described in Refs. [18] and [19]. However, this *collective* transverse cooling relies on the same coupling mechanism, namely Coulomb collisions, responsible for beam heating [11] which poses a fundamental limitation to the achievable transverse emittances. In addition, for dilute ion beams, IBS coupling, and thus indirect transverse cooling, becomes inefficient. In order to overcome these limitations, especially in view of Coulomb ordering, we have recently realized transverse laser cooling based on *single-particle* interaction of the ions with the laser light [14]. This cooling scheme, first suggested by A. Wolf [25], exploits longitudinal-horizontal coupling arising from storage ring dispersion in combination with the transverse gradient of the longitudinal light force arising from the Gaussian laser beam profile. Thus, damping of the longitudinal momentum fluctuations is transferred to the horizontal degree of freedom. True 3D cooling is achieved by additionally mixing horizontal and vertical motion through betatron coupling. Although interacting only longitudinally with the ion beam, laser light can therefore efficiently cool a stored ion beam in all three dimensions to very high phase-space densities.

C Diagnostics at the TSR

The longitudinal density distribution of the ion bunches can be probed by an electrostatic pickup system (see Fig. 1). The system measures the voltage induced by the ion current on a capacitor consisting of two metal plates. Any temporal change in the induced voltage is proportional to the change of the ion current. Given the revolution frequency of the ions one can therefore directly deduce the longitudinal ion distribution from the pickup signal. The longitudinal velocity distribution is determined by ramping a bias voltage applied to drift tubes in the laser-cooling section and detecting the intensity of the fluorescence light from the cooling laser. Since the local velocity of the ions inside the drift tube is proportional to the applied voltage, the fluorescence spectrum as a function of the bias voltage can be interpreted as the Doppler spectrum of the velocity distribution [9].

When no voltage is applied to the drift tubes, the fluorescence signal is proportional to the number of atoms in a small velocity interval ($\simeq 50\,\mathrm{m/s}$) around the mean velocity because of the resonant character of the laser-ion interaction. The drift tubes can also be used to implement the extension of the light-force capture range as described above [21]. In this case, the fluorescence signal yields the amount of ions undergoing the rapid adiabatic passage, i.e. ions with large deviations ($\lesssim 1000\,\mathrm{m/s}$) from the mean velocity. Since such large deviation are caused by close Coulomb collisions, the fluorescence signal from the capture range extension provides a measure of the probability of these collisions.

Transverse emittances are measured by a beam profile monitor (BPM) schematically indicated in Fig. 1. The BPM spatially resolves ions produced by collisions of the ion beam with residual gas. From the Gaussian spatial distribution of the ion beam at the BPM position one can deduce the horizontal and vertical emittances from the known lattice functions of the storage ring [9].

III NOVEL BUNCH FORMS AND SPACE-CHARGE EFFECTS

The standard technique for creating bunched beams consists in applying a longitudinal electric field oscillating at some harmonics h of the revolution frequency. This can be accomplished by, e.g., feeding an RF voltage of some tens of volts amplitude (approx. 30 dBm power) to the longitudinal kicker plates shown in Fig. 1 or to a resonator. The longitudinal pseudopotential experienced by the ions is proportional to the applied voltage leading to sinusoidal bunch potentials in the comoving frame. The longitudinal ion density distribution in such a sinusoidal potential is strongly inhomogeneous. For some applications, in particular the formation of Coulomb-ordered ion beams, a spatially homogeneous distribution of the laser-cooled beam would be preferable.

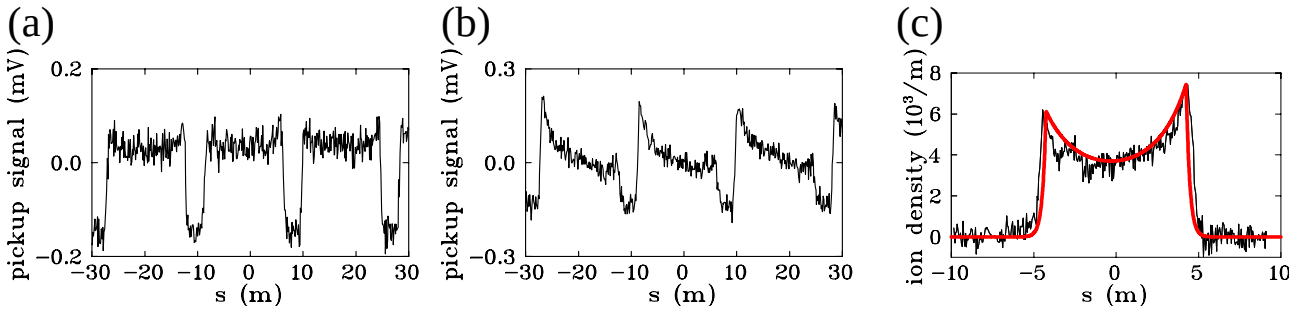

FIGURE 3. (a) Pickup signal of a square-well bunch versus the longitudinal coordinate in the comoving frame. The pickup signal reflects the density distribution of ions. The beam is bunched at the third harmonics ($\nu_b = 676\,\mathrm{kHz}$) of the revolution frequency with a duty-cycle of 80%. Stable velocity and synchroneous velocity are prefectly matched. In the thermal regime, the rectangular shape of the distribution directly reflects the potential form. (b) Density distribution under the same conditions as in (a) but with the bunch frequency decreased by only 2 Hz. (c) Longitudinal density distribution of an ion ensemble in the space-charge regime at a duty cycle of 50%. The distribution exhibits strong effects of Coulomb repulsion. The result of a model calculation is shown by the solid line on the experimental data.

We have therefore developed a method which combines homogeneous ion distributions as in a coasting beam with the longitudinal ion confinement in buckets for the suppression of IBS cooling losses.

A Square-well bunch potentials

For homogeneous ion distributions inside the bunch, a square-well potential is required. Since the bunch potential in the comoving frame is proportional to the applied voltage, this can readily be realized by applying a voltage with rectangular waveform. A particularly nice feature of rectangular bunch potentials is the possiblity to externally adjust the length of the bunch, and thus the longitudinal density, by simply changing the on/off-ratio (duty cycle) of the applied rectangular wave. To exclude distortions of the potential due to the limited bandwidth of our RF amplifier, we have used the third harmonics ($h = 3$) of the revolution frequency for our experiments ($\nu_b = 676\,\mathrm{kHz}$). The counterforce to the light-pressure force is generated by a sawtooth wave at the same frequency which is added phase-coherently to the voltage. In the comoving frame of the ions, one thus creates a potential well with a bottom of constant slope [b] as schematically depicted in Fig. 2 (b). The resulting counterforce is constant, independent of the ion velocity. The sum of light-pressure force and counterforce can be linearly expanded as $F \approx -\alpha(v - v_*)$ with α denoting the friction coefficient and v_* the velocity at stable force equilibrium (see Fig. 2 (a)). Ions are cooled towards the stable velocity, which depends on the counterforce and the laser intensity as does the friction coefficient.

To create constant ion density in the bucket, one has to achieve force equilibrium at the synchoneous velocity $v_s = C\nu_b/h$ which is determined by the bunch frequency ν_b (C = ring circumference). Therefore, the stable velocity v_* has to be exactly matched with the synchroneous velocity . An experimental realization of a constant longitudinal density distribution is presented in Fig. 3 (a). If the two velocities are unequal, the ions experience a constant net force $F \approx -\alpha(v_* - v_b)$. This force will push them towards one end of the potential well yielding density distributions as shown in Fig. 3 (b).

B Space-charge effects

At large longitudinal temperatures [c] and low densities, one can neglect the energy associated with the mutual interaction of the ions due to Coulomb repulsion (*thermal regime*). The longitudinal density distribution is

---

[b] Typical ramp slopes are 10 V/μs corresponding to ring-averaged counterforces around 3 meV/m.

[c] Due to the bimodal character of the longitudinal velocity distribution, it is, strictly speaking, not appropriate to ascribe a temperature to the ensemble. In the context here, temperature is meant as a measure of the mean kinetic energy of the ions in the frame moving at the mean ion velocity.

determined by a Boltzmann distribution in the pseudopotential which includes the combined action of bunching fields, light-pressure force, and a term associated with a possible mismatch between equilibrium velocity and synchroneous velocity. Density distributions observed in the thermal regime are shown in Fig. 3 (a) and (b).

The bimodal character of the velocity distribution can be accounted for by assuming two different temperatures for the two subensembles. Since v_* represents the velocity at force equilibrium between light-pressure force and counterforce, the cold partition of the ions interacts with a pure square-well potential. The hot fraction of the ion velocity distribution is far detuned from resonance with the laser light. The counterforce is not balanced by the light pressure force leading to an asymmetric ion distribution in the bucket. However, because the large temperature of the hot partition, the energy gain related to the counterforce is generally much smaller than the thermal energy. The asymmetry of the distribution is therefore not very pronounced as can be inferred from Fig. 3 (a).

As the longitudinal temperature gets lower and the density increases, the influence of the ionic space-charge on the density distribution becomes important (*space-charge regime*). Qualitatively, the repulsive electrostatic force between the ions will push them to the edges of the potential well which leads to density distributions as shown in Fig. 3 (c). Space-charge effects have been observed before in sinusoidal buckets [17,26], and models have been introduced to describe these space-charge dominated bunches [26–28]. The models are based on a mean-field Coulomb potential proportional to the *local* ion density. From the condition that, in equilibrium, the mean field energy has to compensate the external potential, these models predict a constant ion density for square-well buckets, in contradiction to the experimental data. In square-well potentials, the local-density approximation for the Coulomb potential has to be given up, and the potential has to be calculated *self-constistently* taking into account the external confining forces, the Coulomb interaction and the thermal motion at finite temperatures.

To adequately describe our experimental findings, we have developed a novel approach [29] based on a thermodynamic mean-field model first introduced by Debye and Hückel for ionic solutions. The mean longitudinal Coulomb potential in this model is derived self-consistently from a Poisson-Boltzmann equation [30]. The density distribution is calculated by the second derivative of the Coulomb potential with respect to the longitudinal coordinate. A comparison between a measured ion distribution and the model calculations is presented in Fig. 3 (c). The model has no free parameters, since all relevant parameters, like beam current and temperatures of the two subensembles, are determined experimentally. From the comparison between model and experiment, we can infer that only the cold partition of the velocity distribution contributes to the density enhancement at the potential edges. The apparant asymetry of the density distribution stems from the interaction of the the cold partition with the slightly asymetric distribution of the hot ions experiencing the counterforce. As mentioned above, the asymmetry of the hot distribution is small, yet it creates a measurable effect through the Coulomb interaction with the cold partition.

IV ANOMALOUS BEAM BEHAVIOUR

When the thermal energy per ion becomes smaller than the Coulomb potential energy between two neighboring ions ($\Gamma \gtrsim 1$), the ions start to show ordering phenomena. The ion configuration representing the energetic ground state sensitively depends on the local ion density. Based on Molecular Dynamics for cylindrically confined ion plasmas, Hasse and Schiffer have derived stability ranges for particular ion structures as a function of the linear particle density [31]. At low enough densities and $\Gamma \simeq 1$, the ions are ordered in a linear Coulomb string ("1D crystal"). As the density is increased and $\Gamma \gg 1$, the ions evade into the transverse directions to form 2D or 3D crystalline structures. The transition to different ordered structures as a function of the linear density has been observed in linear ion traps nicely confirming the predictions of Hasse and Schiffer [2,3].

In storage rings like the TSR, a 1D Coulomb string and possibly a vertical zig-zag band are predicted to represent the only stable configurations [32]. Three-dimensional structures are excluded due to shear and other destructive effects exerted by the ring lattice. The simulations suggest that the longitudinal laser cooling rates achievable with bunched beams should suffice to generate a linear Coulomb string. In addition, the Hasse-Schiffer stablity analysis tells one, that the mean distance between adjacent ions must become smaller than a critical value ($d_{crit} \gtrsim 30\,\mu$m) to guarantee that the linear string represents the ground state. At higher linear densities, stable Coulomb structures are excluded in the TSR. The homogeneous ion distribution achieved in square-well buckets ensures that the Hasse-Schiffer condition of minimum ion distance is fulfilled over the whole bunch length. This is why square-well buckets are more advantageous than sinusoidal ones. Single-particle transverse cooling as described in Sect. IIB has to be applied since, at the required low densities, collective

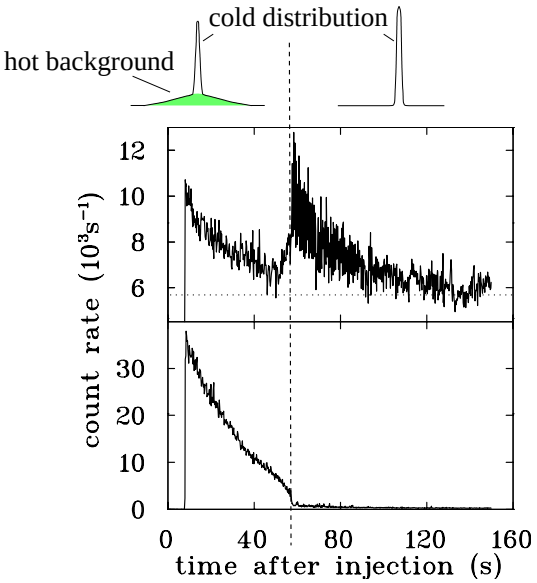

FIGURE 4. Temporal behaviour of the ion fluorescence during laser cooling. Longitudinal velocity distributions are schematically depicted on top of the figure. Upper trace: signal from the cold ion distribution (the dotted line indicates the straight light background). Lower trace: signal from the hot ion background. Laser cooling starts at $t = 8\,\mathrm{s}$. At $t \approx 60\,\mathrm{s}$ the hot background suddenly disappears, as seen from the lower trace, and the fluorescence emitted by the cold fraction of ion increases by nearly an order of magnitude.

transverse cooling through IBS becomes inefficient.

A Recent obervations

In a very recent series of experiments, we have investigated laser cooling in square-well buckets in combination with single-particle transverse cooling. The bunch frequency is adjusted such that the stable velocity is exactly matched with the synchroneous velocity to achieve a homogeneous density distribution in the bucket. The duty cycle is set to 50%, and the capture range extension of the laser force (see Sect. II A) is applied to one pair of the HV drift tubes. As explained in Sect. II C, we can record different fluorescence signals providing information on the longitudinal velocity distribution of the ions, the fraction of cold ions, and the rate of intrabeam collisions. We measure these fluorescence signals as a function of time during the decay of the number of stored ions through rest gas collisions.

A typical example of a single time scan is presented in Fig. 4. Quite surprisingly, at about 60 s after ion injection intrabeam collisions suddenly vanish, and the fraction of cold atoms drastically increases. At the same time, the hot background of ions disappears, and the longitudinal temperature of the cold partition drops from some Kelvin to $T \approx 1\,K$. Thus, the ion distribution changes into a state where all ions gather in a narrow velocity interval around the stable velocity without further undergoing hard Coulomb collisions.

Such behaviour can be perfectly reproduced in subsequent injections, but depends extremely critical on the bunch frequency, i.e. the matching between synchroneous velocity and stable velocity [d]. When, after the transition has occured, the bunch frequency is switched to a value differing by some Hz from the matched frequency, collisions and the hot background reappear. They dissappear again when the bunch frequency is switched back to its original value after some seconds. We have also shuttered the laser beam for several seconds after the disappearance of collisions. During this time interval we can naturally observe no fluorescence light. But when the laser is turned on again, again no indication for collisions or a background of hot ions is found.

---

[d] The dependence on the bunch frequency, and thus on the exact revolution frequency of the ions, is so critical (on the level of 10^{-6}) that we are limited by the stability of the storage ring magnets.

B Interpretations

Our observations show strong similarities with the anomalous longitudinal temperature reduction in dilute beams of electron-cooled, highly-charged ions at the GSI as reported by M. Steck *et al.* [33]. As an important difference, we observe the sudden disappearance of IBS heating at mean distances between the particles which are 3 orders of magnitude smaller than in the GSI experiments. All signatures we have observed so far are consistent with the formation of a Coulomb ordered structure. The transition occurs typically after 2.5 beam lifetimes when about 10^6 ions are left in the ring. The fact, that no transition occurs at larger particle numbers, i.e. smaller average particle spacings, could be interpreted in terms of the stability criterion by which the ion spacing has to be above the critical value $d_{\rm crit}$ to exclude unstable higher-dimensional Coulomb-ordered structures (see discussion above). The mean distance of some tens of μm, at which the transition happens, is consistent with predictions for the formation of a Coulomb string [31] as calculated with the actual TSR parameters [32]. The same holds for the temperature: At the transition we estimate from our data a longitudinal plasma parameter $\Gamma_{\|} \equiv e^2/(4\pi\varepsilon_0 a k_B T_{\|}) \approx 1$ ($2a$ = average longitudinal particle distance, $T_{\|}$ = longitudinal temperature). Once ordering is achieved, hard Coulomb collisions are suppressed [11,13] which would explain the lower trace in Fig. 4. Due to the reduction of this heating mechanism, the mean kinetic energy of the ion ensemble in the comoving frame is strongly decreased. Furthermore, the stability of an ion crystal should very critically depend on the bunch frequency due to the additional forces arising from a velocity mismatch (see Sect. III A), in agreement with the observed behaviour.

However, all our observations refer only to the longitudinal dynamics. Due to the limited resolution of our BPM (beam emittances $\gtrsim 10^{-3}\,\pi$ mm mrad) and the poor statistics at the low particle numbers, we can make no definite statement on the transverse beam dynamics. Strong heating of the transverse motion would lead to the disappearance of hard Coulomb collisions which would then result in signals similar to the ones shown in Fig. 4. A blowup of the transverse motion, however, would not be reversible after changes in the bunch frequency, as we know from experiments on transverse heating on coupling through ring dispersion [14]. In some preliminary measurements on the transverse degree of freedom we could also find no evidence for a dramatic transverse beam blowup. The observed disappearance of hard Coulomb collisions might alternatively indicate transverse beam instabilites. Possible sources of such transverse instabilities could be space-charge induced tune shifts [34] or transverse action of the light pressure force via higher-order longitudinal-transverse coupling processes through, e.g., the ring chromaticity. Such instabilites competing with laser cooling might possibly lead to an increase of the transverse phase-space, and thus to the observed disappearance of IBS, without necessarily resulting in a dramatic blowup of the beam. At the present stage of our analysis neither of the possibilities, beam crystallization or transverse instabilities, can be definitely proven or ruled out.

V CONCLUSIONS

The quest for crystalline beams of fast ions has entered a decisive phase. Recent achievements in laser cooling at storage rings, in particular the realization of a single-particle transverse cooling mechanism [14] and the introduction of quasi-coasting bunched beams confined in square-well buckets, have opened an intriguing new regime for the investigation of cold and dense ion beams. We have found clear evidence for a sudden disappearance of hard Coulomb collisions at longitudinal temperatures around 1 K. The transition occured when the mean distance between the ions became larger than some tens of μm. Our observations are consistent with expected features of Coulomb ordering, but they might possibly also be explained by longitudinal-transverse decoupling through transverse beam instabilities. Our limited knowledge on the dynamics of the transverse degree of motion does, at present, not allow us to experimentally distinguish between these two processes. We need further experiments, with improved diagnostics on the transverse degree of freedom, to unambiguously interpret our observations. The next laser cooling beam times at the TSR are awaited with tension and will certainly lead to further clarification.

ACKNOWLEDGEMENTS

We thank T. Schätz and C. Podlech for their support during beam times. Stimulating discussions with A. Wolf and H.-J. Miesner are greatfully acknowledged, as well as invaluable technical contributions by H. Krieger.

REFERENCES

1. Diedrich, F., *et al.*, *Phys. Rev. Lett.* **59**, 2931 (1987); Wineland, D.J., *et al.*, *ibid.*, 2935 (1987).
2. Birkl, G., Kassner, S., Walther, H., *Nature* **357**, 310 (1992).
3. Drewsen, M., *et al.*, *Phys. Rev. Lett.* **81**, 2878 (1998).
4. See contribution by J.J. Bollinger *et al.* in this volume for an overview on crystalline one-component plasmas.
5. Habs, D., and Grimm, R. , *Annu. Rev. Nucl. Part. Sci.* **45**, 391 (1995), and references therein.
6. For a recent overview on crystalline beams see Maletic, D.M., and Ruggiero, A.G., (eds.) *Crystalline Beams and Related Issues*, Singapore: World Scientific, 1996.
7. Schröder, S., *et al.*, *Phys. Rev. Lett.* **64**, 2901 (1990).
8. Hangst, J.S., *et al.*, *Phys. Rev. Lett.* **67**, 1238 (1991).
9. Petrich, W., *et al.*, *Phys. Rev. A* **48**, 2127 (1993).
10. Bosser, J., (ed.), *Proc. of the Workshop on Beam Cooling and Related Topics*, CERN Report 94-03, 1994.
11. Seurer, M., Reinhard, P.-G., Toepffer, C., *Nucl. Instr. Meth. Phys. Res. A* **351**, 286 (1994); Spreiter, Q., Seurer, M., Toepffer, C., *ibid.* **364**, 239 (1995); Seurer, M., Spreiter, Q., Toepffer, C., in Ref. [6], p. 311;
12. Schiffer, J.P., in Ref. [6], p. 217, and references therein.
13. Wei, J., Okamoto, H., Sessler, A.M., *Phys. Rev. Lett.* **80**, 2606 (1998); see also Wei, J., *et al.*, in Ref. [6], p. 229.
14. Lauer, I., *et al.*, *Phys. Rev. Lett.* **81**, 2052 (1998).
15. A discussion of both methods is presented by Grimm, R., *et al.*, in *Proc. of the Workshop on Quantum Aspects of Beam Physics*, Monterey, 1998, to be published.
16. Metcalf, H., and van der Straten, P., *Phys. Rep.* **244**, 203 (1994).
17. Hangst, J.S., *et al.*, *Phys. Rev. Lett.* **74**, 4432 (1995).
18. Miesner, H.-J., *et al.*, *Phys. Rev. Lett.* **77**, 623 (1996)
19. Miesner, H.-J., *et al.*, *Nucl. Instrum. Meth. Phys. Res. A* **383**, 634 (1996).
20. Atutov, S.N., *et al.*, *Phys. Rev. Lett.* **80**, 2129 (1998).
21. Wanner, B., *et al.*, *Phys. Rev. A* **58**, 2242 (1998).
22. Channel, P.J., *J. Appl. Phys.* **52**, 3791 (1981).
23. De Salvo, L., Bonifacio, R., Barletta, W., *Opt. Comm.* **116**, 374 (1995).
24. Calabrese, R., *et al.*, *Opt. Comm.* **123**, 530 (1996).
25. Wolf, A., "Transverse cooling of a stored ion beam in a collinear laser beam", presented at the 2nd Workshop on Diagnostics of Laser Cooled Beams, Sandbjerk, Denmark, 1991.
26. Ellison, T.J.P., *et al.*, *Phys. Rev. Lett.* **70**, 790 (1993).
27. Reiser, M., and Brown, N., *Phys. Rev. Lett.* **71**, 2911 (1993).
28. Nagaitsev, S.S., *et al.*, in Ref. [10], p. 405.
29. A detailed description of the model and the comparison with experiments is going to published elsewhere: Eisenbarth, U., *et al.*, in preparation.
30. Cambel, A.B., and Shapiro, A.H., *Real Gases*, New York: Academic Press, 1963.
31. Hasse, R.W., and Schiffer, J.P., *Ann. Phys. (N.Y.)* **203**, 419 (1990).
32. Wei, J., Li, X.P., Sessler, A.M., in *Proc. of the Particle Accelerator Conf. and Int. Conf. on High-Energy Accelerators*, 1995, p. 2946.
33. Steck, M., *et al.*, Phys. Rev. Lett. **77**, 3803 (1996).
34. Bryant, P.J., and Johnson, K., *The Principles of Circular Accelerators and Storage Rings*, Cambridge: Cambridge University Press, 1993.